

ДИНАМИКА КОНСТРУКЦИЙ И СООРУЖЕНИЙ

UDC 626.624.04

DOI: 10.22363/1815-5235-2019-15-2-158-168

RESEARCH PAPER

Static and dynamic analyses of the heightening of concrete face gravel dam Limon (Peru)

Yury P. Lyapichev

JSC “Institute Hydroproject”, 2 Volokolamskoe Shosse, Moscow, 125993, Russian Federation,
International Commission on Large Dams (ICOLD), 61 Avenue Kleber, Paris, 75016, France

Received: January 11, 2019

Revised: March 12, 2019

Accepted: March 22, 2019

Keywords:

concrete face gravel dam (CFGD);
nonlinear dynamic analysis;
ground acceleration;
earthquake accelerogram;
seepage analysis

Abstract

Aims of research. Expert validation of all proposed design solutions, development of necessary design solutions for the heightening of the Limon dam according to the ICOLD recommendations.

Methods. The detailed static and seismic (dynamic) analyses of stress-strain state and seepage of concrete face rockfill dam Limon (Peru) were performed using the advanced software FLAC-3D (USA) and PLAXIS 2D (Holland), respectively. The elasto-plastic model with Mohr – Coulomb criterion with variable shear angles of gravel and pebble zones of dam materials and its foundation soils was used in the static and seismic (dynamic) analyses of the dam. The dynamic nonlinear analyses of stress-strain state of two variants of Limon dam with full reservoir under Maximum Credible Earthquake (MCE) action of the Mar–Chile Earthquake accelerogram.

Results. On the base of these analyses the recommendations were developed for the project of the dam heightening from 43 up to 82 m before the initial filling of the reservoir. Expert validation of all proposed design solutions, necessary design solutions for the heightening of the Limon dam were developed according to the ICOLD recommendations.

Introduction

In July 2012 the Government of Lambayeque province (Peru) invited the author of this article as an international expert and member of ICOLD to perform the expert validation of design of the heightening of concrete face gravel dam (CFGD) Limon from 43 to 82 m. The dam is the main element of project “Proyecto Especial Olmos – Tinajones (PEOT)”. The hydraulic transfer scheme of

the project includes the TransAndes water-transfer 26 km long tunnel now completed. The 82 m high Limon CFGD is located on the right bank of Huancabamba river in remote region of Andes with very high seismicity. Maximum Credible Earthquake (MCE) with the return period $T = 5000$ years and $A_{\max} = 0.57g$ corresponds to ICOLD recommendations: Bulletins 148, 122, 154, 155, 167 [1–5] and was much more dangerous than adopted in 2009 Brazilian design: $A_{\max} = 0.39g$, $T \approx 1000$ years [6].

In the first PEOT project, developed by Hydroproject Institute (Moscow) in 1982, the variant of 82 m high Limon rockfill dam with clay core

© Lyapichev Yu.P., 2019



This work is licensed under a Creative Commons Attribution 4.0 International License

was adopted for the one-stage dam construction. But later due to the political and financial problems in Peru the project implementation was delayed for 20 years and was resumed as a two-stage construction by BOT scheme (build, operate and transfer to owner), proposed by Odebrecht construction company (Brazil). The company changed the Soviet design of one-stage 82 m high Limon traditional rockfill dam with clay core in favor of the two-stage CFGD (43 and 82 m high). The Soviet project of shore spillway remained unchanged.

1. Seepage analysis of Limon CFGD ($H = 82$ m) and its alluvial (40 m deep) foundation

Seepage analysis was made using the software PLAXIS 2D PlaxFlow (The Netherlands) [7].

In figure 1 is presented the geometry of dam with zones of materials and its 40 m deep alluvial strata of foundation in channel section 10–10' and their permeability coefficients. In figure 2 is presented the finite element mesh of dam and its foundation in channel section 10.

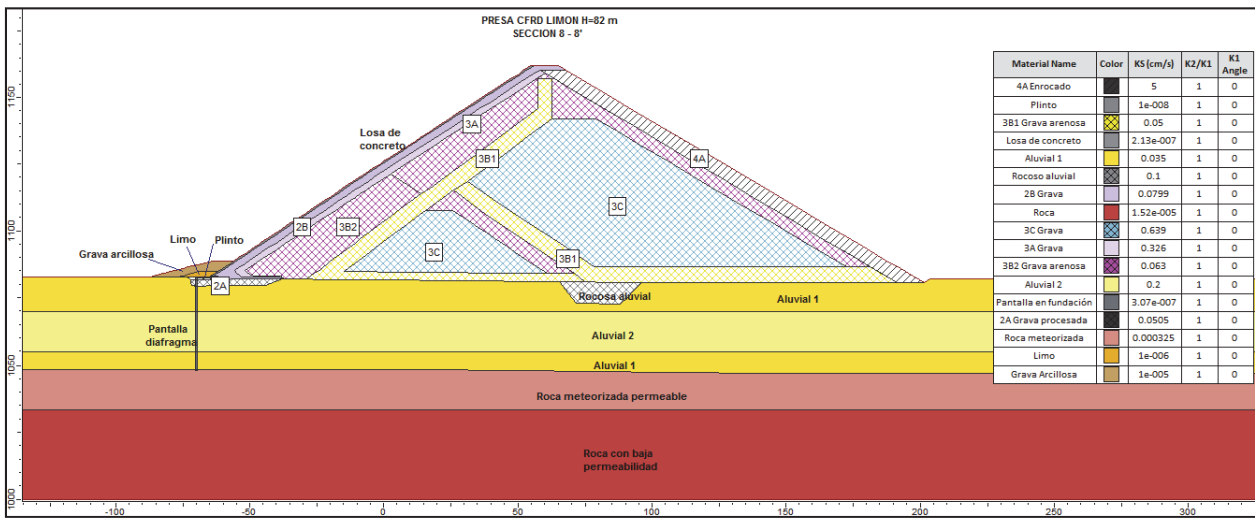


Figure 1. Zoning and permeability of soils of CFGD Limon $H = 82$ m and its foundation in channel section

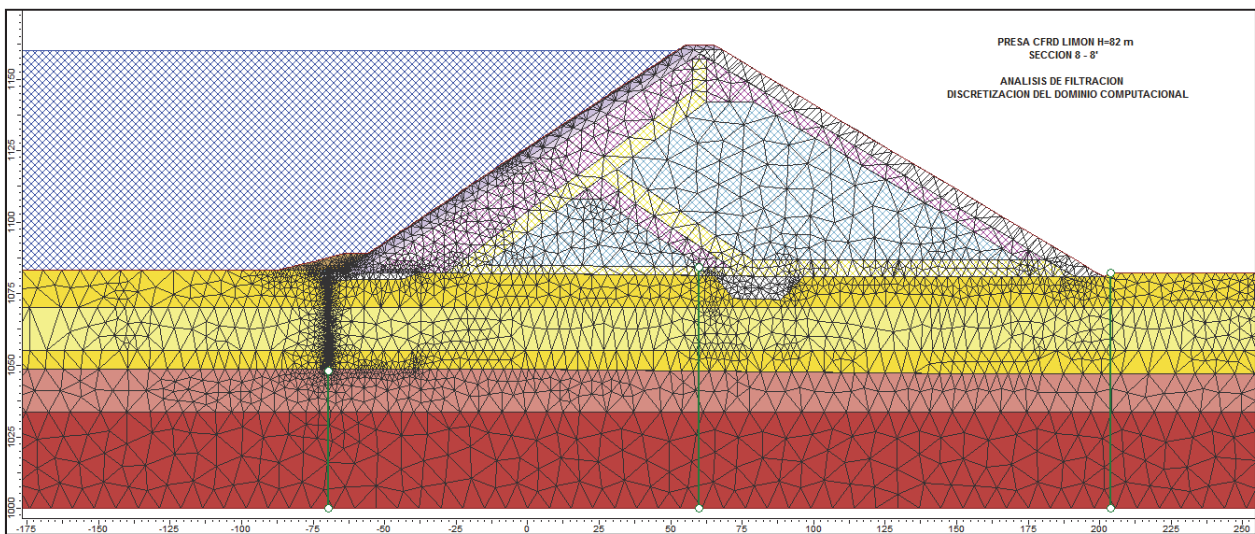


Figure 2. Finite element mesh of CFGD Limon $H = 82$ m and (40 m deep) foundation in channel section

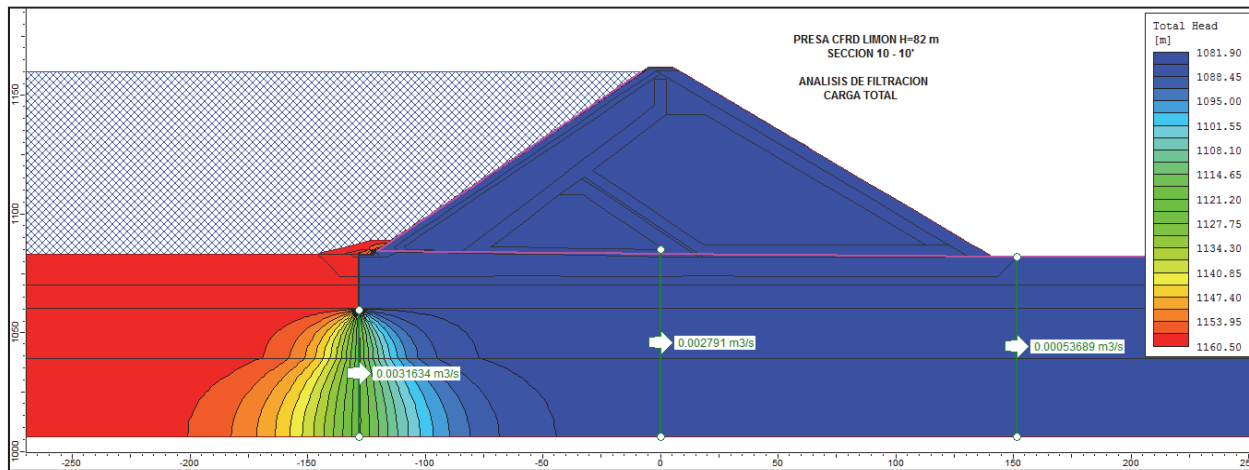


Figure 3. Equipotential lines of the total seepage heads in rock foundation below the concrete diaphragm

The results of the equipotential lines of total seepage heads in the rock foundation below the plastic concrete diaphragm are showed in figure 4, verifying the significant reduction of the total seepage and pressure heads in the rock foundation by effect of the plastic concrete diaphragm in foundation.

Table 1 shows the unit seepage flows in the dam foundation for construction stages of $H = 43$ m and

$H = 82$ m in sections 8–8' (in right abutment) and 10–10' (channel section) below the concrete diaphragm, in the central dam axis and below the dam toe. The relationship of unit seepage flows in section 8–8' and 10–10' shows that seepage flow in the foundation of the dam $H = 82$ m would be more than twice the seepage flow in the foundation of the dam $H = 43$ m.

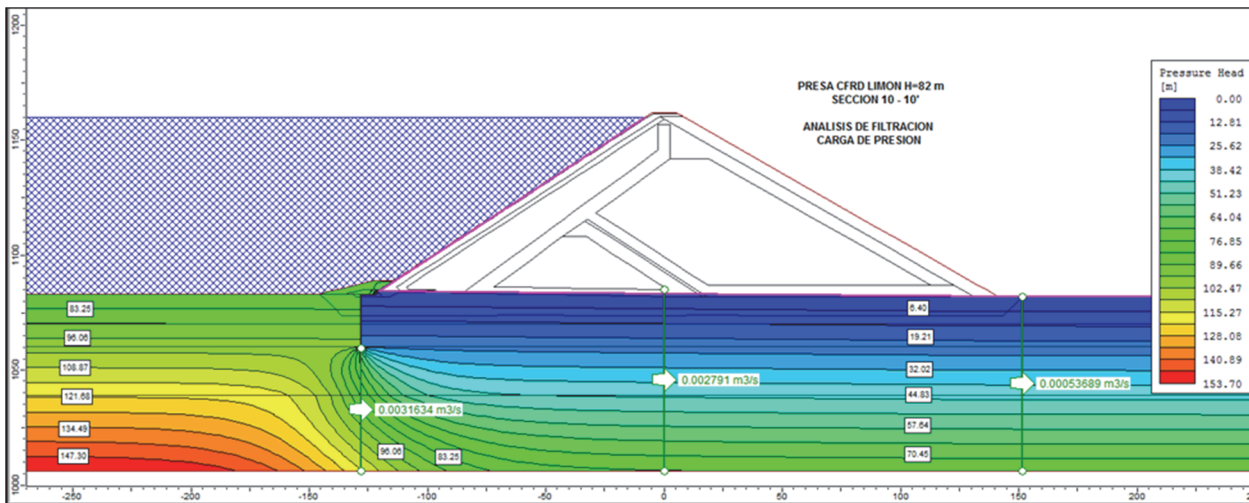


Figure 4. Equipotential lines of seepage pressure heads in rock foundation below the concrete diaphragm

Table 1

Unit seepage flows in the dam foundation for construction stages of $H = 43$ m and $H = 82$ m

Dam	Section	Unit seepage flows ($m^3/s/m$)		
		Below concrete diaphragm	In axis of dam cross-section	Below toe of downstream slope
I Stage $H = 43$ m	8–8'	1.373×10^{-3}	1.37×10^{-3}	0.744×10^{-3}
	10–10'	1.495×10^{-3}	1.38×10^{-3}	0.652×10^{-3}
II Stage $H = 82$ m	8–8'	2.865×10^{-3}	2.759×10^{-3}	1.904×10^{-5}
	10–10'	3.163×10^{-3}	2.791×10^{-3}	0.536×10^{-3}
Relation Q_{H82}/Q_{H43}	8–8'	2.09	2.01	2.56
	10–10'	2.12	2.02	0.82

2. Seismic (dynamic) analysis of 82 m high Limon CFGD under MCE action ($A_{max} = 0.57 g$)

The main results of dynamic nonlinear analysis of stress-strain state of Limon CFGD ($H = 82 m$, adopted variant 2 with additional downstream rock-fill zone) with full reservoir under Maximum Credible Earthquake (MCE) action of the Mar–Chile Earthquake accelerogram are given in figures 5–17. The previous dynamic analysis of variant 1 (without this downstream rockfill zone) are omitted.

Another MCE of the Lima–Peru Earthquake accelerogram was considered also in the dynamic analysis, but its action was less dangerous than that of the Mar–Chile Earthquake accelerogram.

In figure 5 the accelerogram of Mar–Chile Earthquake normalized to the maximum acceleration of $A_{max} = 0.57g$ is shown. The Mar–Chile Earthquake with the return period $T = 5000$ years and $A_{max} = 0.57g$ corresponds to the recommendations of the ICOLD Bulletins [1–5] and was much more dangerous than adopted in previous (2009) Brazilian design: $A_{max} = 0.39 g$, $T \approx 1000$ years [6].

The static and dynamic analyses of stress-strain state of Limon CFGD ($H = 43$ and $82 m$) were made by FLAC-3D software (USA) [8], which was estimated in ICOLD Congress (Canada, 2003) [9] as one of the best software for dynamic analyses of large rockfill dams including CFRDs. The finite element

model of Limon CFGD ($H = 43$ and $82 m$) with its foundation is shown in the figure 6.

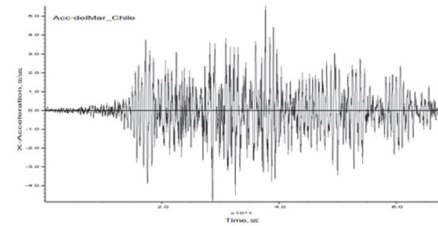


Figure 5. Accelerogram of Mar–Chile

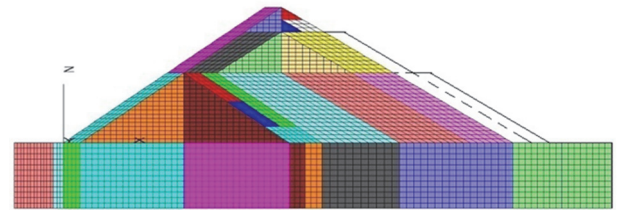


Figure 6. The finite element model of Limon CFGD

Earthquake normalized to $A_{max} = 0.57 g$ ($H = 43$ and $82 m$) with its foundation

Parameters of the elasto-plastic model with Mohr – Coulomb criterion for dam materials and foundation soils in static analyses of Limon CFGD ($H = 43$ and $82 m$) are given in table 2.

Table 2

Parameters of Mohr–Coulomb model in static analyses of Limon CFGD ($H = 43$ and $82 m$)

Numbers and names of zones of dam materials and foundation soils	Material or soils	Dry density and void ratio		Parameters of deformation			Parameters of shear strength of materials	
		$\gamma_{dr}, t/m^3$	n	E (MPa)	Angle of dilatancy (°)	ν	C (MPa)	ψ (°)
1st stage dam ($H = 43 m$)								
1, 3. Foundation	Alluvium	2.15	0.2	108	0	0.30	0	42
2. Diaphragm	Concrete	2.25	0	320	0	0.40	0.4	30
4. Plint slab	Concrete	2.5	0	20000	0	0.17	1.0	60
5. Embankment zone	Gravels and pebbles	2.2	0.15	168	0	0.30	0	46.5
6. Transition zone	Gravels	2.15	0.2	150	10	0.33	0	42
7. Transition zone	Sand	2.1	0.25	100	10	0.33	0	40
8. Concrete face	Concrete	2.5	0	20000	0	0.17	1.0	60
2nd stage dam ($H = 82 m$)								
9. Embankment zone	Gravels	2.2	0.15	168	0	0.30	0	46.5
10. Embankment zone	Gravels	2.2	0.15	168	0	0.30	0	46.5
11. Transition zone	Gravels	2.15	0.2	150	10	0.33	0	42
12. Transition zone	Sand	2.1	0.25	100	10	0.33	0	40
13. Concrete face	Concrete	2.5	0	20000	0	0.17	1.0	60
14. Downstream zone with 2 berms	Pebbles	2.1	0.25	150	0	0.30	0	46.5

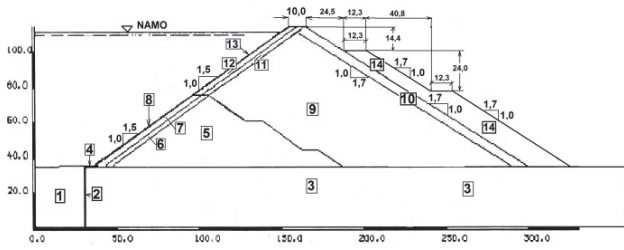


Figure 7. Scheme of CFGD Limon ($H = 42$ and 82 m) (adopted variant with $d-s$ zone 14 with 2 berms)

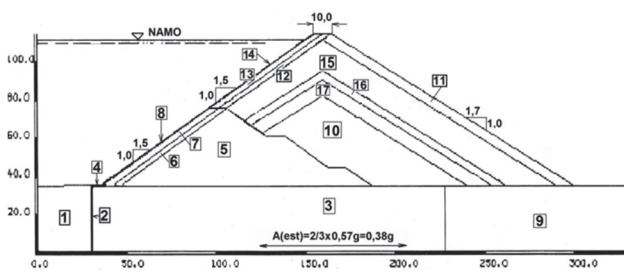


Figure 8. Scheme of CFGD Limon ($H = 43$ and 82 m) with variable shear angles of gravel and pebble zones 10–11, 15–17

Table 3

Values of shear angles of gravel and pebble zones 10–11, 15–17 depending on normal stresses

Normal stresses, σ_n , MPa	0.2	0.5	0.8	1.0	≥ 1.2
Shear angles ψ (°) of gravel and pebble zones	46.5	46.3	42.0	41.1	40.0

Scheme of zoning of CFGD Limon ($H = 82$ m) with variable shear angles of gravel and pebble zones 10–11, 15–17 (figure 8) was used in the pseudo-static analyses of the downstream slope stability under action of the acceleration in dam foundation $A_{hor} = 2/3 \cdot A_{max} = 2/3 \cdot 0.57 g = 0.38 g$.

The distribution of seismic accelerations through the dam height was received according to Russian seismic design norms for dams (SNiP 33-01-2003) using the shear wedge method (figure 9).

Figure 10 shows results of static (the most dangerous circular surface 2) and seismic (the most dangerous circular surface 1) stability of downstream slope of Limon CFGD ($H = 82$ m) taking into account the variable shear angles of gravel and pebble zones 10–11, 15–17. This figure show that the minimum factor of the downstream slope stability under action of seismic loads is more that permissible as per design norms SNiP 33-01-2003 ($F_{min} = 1,22 > F_{perm} = 1,06$) and corresponds to the deep circular sliding surface

between the dam crest and upper alluvial layers of dam foundation.

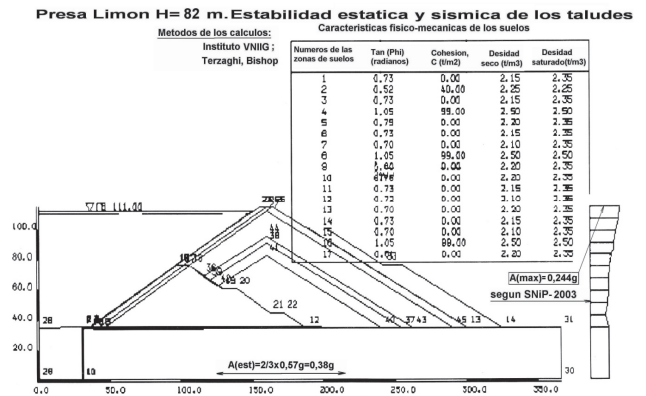


Figure 9. Distribution of seismic accelerations through the dam height ($H = 82$ m) using shear wedge method

Presa Limon $H = 82$ m. Resultados de los calculos estaticos y sismicos por metodo de VNIIG-Terzhagi

Superficie	γ_c	γ_s	$F(\min)$	$F(\text{perm})$
1	280.0	120.0	1,69	1,25
2	290.0	155.0	1,19	1,06

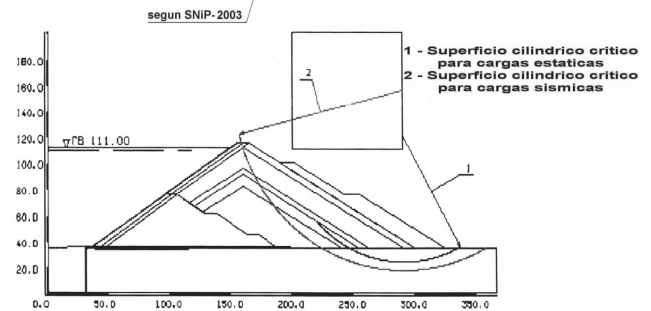


Figure 10. Factors of seismic ($F_{min} = 1,19 > F_{perm} = 1,06$) and static stability ($F_{min} = 1,69 > F_{perm} = 1,25$) of downstream slope

The comparison of results of the seismic stability analysis of the downstream slope of Limon CFGD ($H = 82$ m) with additional pebble zone 14 with two berms (figure 7) with results of the same analysis of the dam but without the additional zone show that the inclusion of this zone in the downstream slope provide a significant increase of the minimum factor of the downstream slope stability from 1.05 up to 1.22. Below in figures 11, 13–15 the main results of dynamic nonlinear analysis of stress-strain state of Limon CFGD ($H = 43$ and 82 m, variant with the additional downstream pebble zone) with full reservoir under action of MCE of the Mar–Chile Earthquake accelerogram are presented. The dam zones with the shear stress state of soils are painted in orange and zones with the tension stress state of soils are painted in blue (figure 11).

Parameters of Mohr–Coulomb model used in the dynamic nonlinear analysis of Limon CFGD ($H = 43$ and 82 m) are given in table 4.

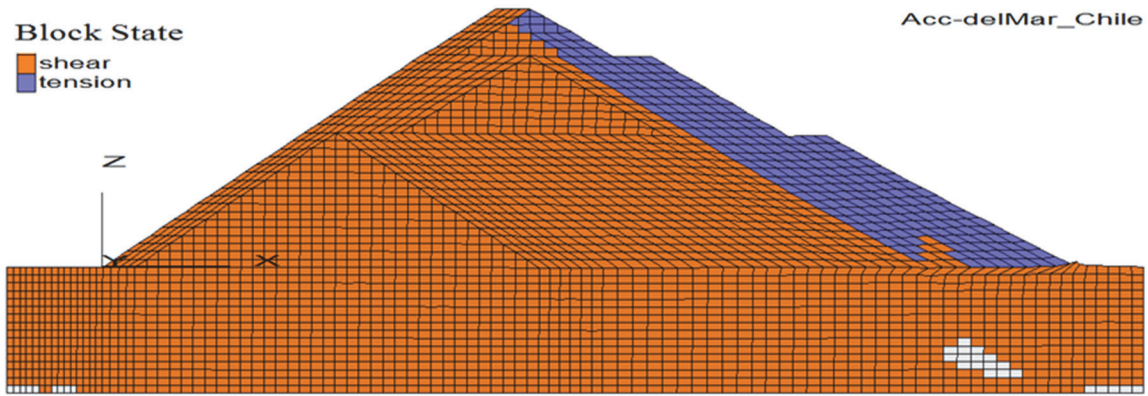


Figure 11. Zones of Limon CFGD ($H = 43$ and 82 m) with the shear and tension stress state of soils under action of SMC of the Mar–Chile Earthquake accelerogram with $A_{max} = 0.57$ g

Table 4

Parameters of Mohr–Coulomb model in dynamic analyses of Limon CFGD ($H = 43$ and 82 m)

Numbers and names of zones of dam materials and foundation soils	Material or soils	Dry density and void ratio		Dynamic modulus of elasticity E^{dyn} , MPa	Shear modulus G_{max} (MPa)	Initial coefficient of damping ξ , %	Reduction of parameters G_{max} and ξ
		γ_{dr} , t/m ³	n				
<i>1st stage dam ($H = 43$ m)</i>							
1, 3. Foundation	Alluvium	2.15	0.2	1300	$G_{max} = 35(\sigma_m)^{0.5}$	5	see figure A
2. Diaphragm	Concrete	2.25	0	1600	$G = E^{dyn} / [2(1 + \nu)]$	3	–
4. Plint slab	Concrete	2.5	0	20000	$G = E^{dyn} / [2(1 + \nu)]$	2	–
5. Embankment zone	Gravels and pebbles	2.2	0.15	2000	$G_{max} = 40(\sigma_m)^{0.5}$	5	see figure A
6. Transition zone	Gravels	2.15	0.2	1000	$G_{max} = 22(\sigma_m)^{0.5}$	4	see figure A
7. Transition zone	Sand	2.15	0.2	700	$G_{max} = 20(\sigma_m)^{0.5}$	4	see figure A
8. Concrete face	Concrete	2.5	0	20000	$G = E^{dyn} / [2(1 + \nu)]$	5	–
<i>2nd stage dam ($H = 82$ m)</i>							
9. Embankment zone	Gravels	2.2	0.15	2000	$G_{max} = 40(\sigma_m)^{0.5}$	5	see figure A
10. Embankment zone	Gravels	2.2	0.15	2000	$G_{max} = 40(\sigma_m)^{0.5}$	5	see figure A
11. Transition zone	Gravels	2.15	0.2	1000	$G_{max} = 22(\sigma_m)^{0.5}$	4	see figure A
12. Transition zone	Sand	2.1	0.25	700	$G_{max} = 20(\sigma_m)^{0.5}$	4	see figure A
13. Concrete face	Concrete	2.5	0	20000	$G = E^{dyn} / [2(1 + \nu)]$	5	–
14. Downstream zone with 2 berms	Pebbles	2.15	0.2	1500	$G = E^{dyn} / [2(1 + \nu)]$	5	see figure A

Note: (σ_m) – medium stress (effective) in kPa.

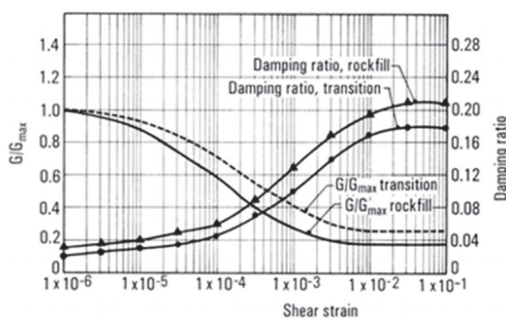


Figure 12. Curves of reduction of the shear modulus G/G_{max} and initial coefficient of damping ξ , % of soils of the dam and its foundation

Under action of the Mar–Chile Earthquake the dam would suffer elasto-plastic deformations with large plastic displacements in the wide zone of the downstream slope (figure 13). The large plastic deformations modified the dynamic stress-strain state of the dam and its foundation (figures 13–14). The horizontal and vertical displacement in the dam after the Mar–Chile Earthquake in the upper part of the downstream slope are, respectively, 2.0 and 1.0 m; in the upper berm – 2.2 and 1.1 m; in the lower berm – 2.5 and 1.3 m and at the toe of the slope – 6.0 m and zero (figure 13). The intensity of shear deformations (figure 13) is concentrated in the narrow zone in lower part of dam downstream slope.

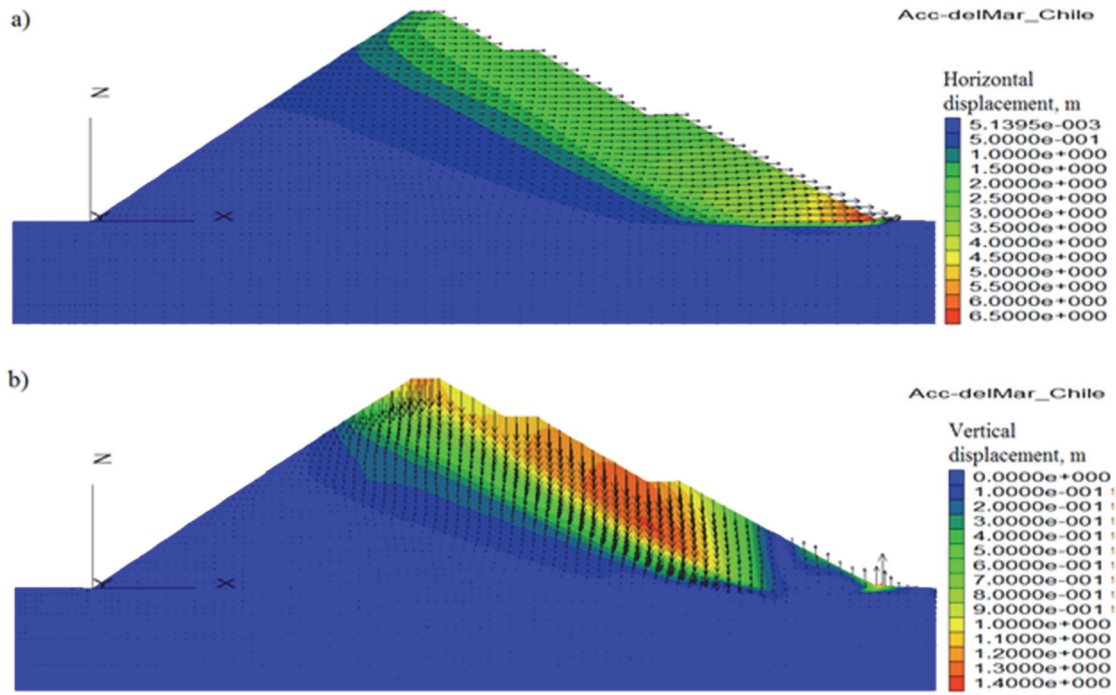


Figure 13. Horizontal (a) and vertical (b) displacements in Limon dam (82 m) after Mar–Chile Earthquake

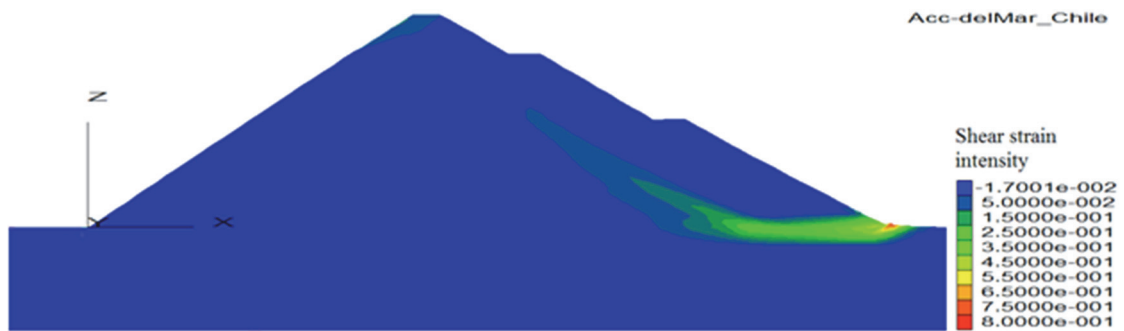


Figure 14. Intensity of the shear deformations in Limon dam (82 m) after the Mar–Chile Earthquake

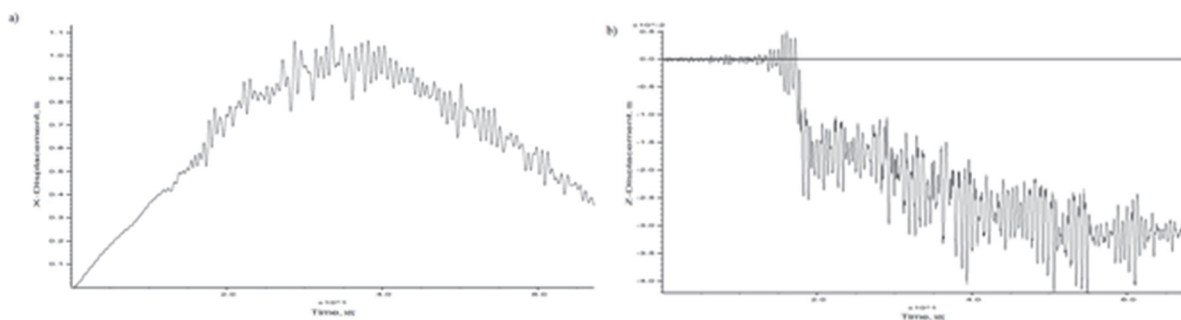


Figure 15. The time history of the residual horizontal (a) and vertical (b) displacements of the crest of Limon dam (82 m) during the Mar–Chile Earthquake

The time history of the residual horizontal (a) and vertical (b) displacements of the dam crest during the Mar–Chile Earthquake is shown in figure 15.

The maximum horizontal and vertical displacements of the dam crest during the Mar–Chile Earthquake are, respectively, 1.5 and 1.1 m.

3. Results of analysis of the concrete face

These results are showed in figure16 and 17 (Limon dam, the 2nd stage, $H = 82$ m). The displacements, bending moments and longitudinal forces (axial) in the concrete face are presented for action of Maximum Credible Eartquake (MCE) of Mar–Chile after filling of the reservoir up to maximum elevation (Limon dam, the 2nd stage, $H = 82$ m). It's shown that the greatest

influences on the concrete face is axial compression, being of lesser bending moment value, therefore, the concrete face will be in compression state. With the dimensions of concrete face, adopted forces and moments it can determine the bearing capacity and reinforcement of thick 0.55 and 0.42 m concrete face based on the diagram of interaction force-bending. Also this reinforcement is also recommended to absorb stresses due to shrinkage and thermal changes in concrete face.

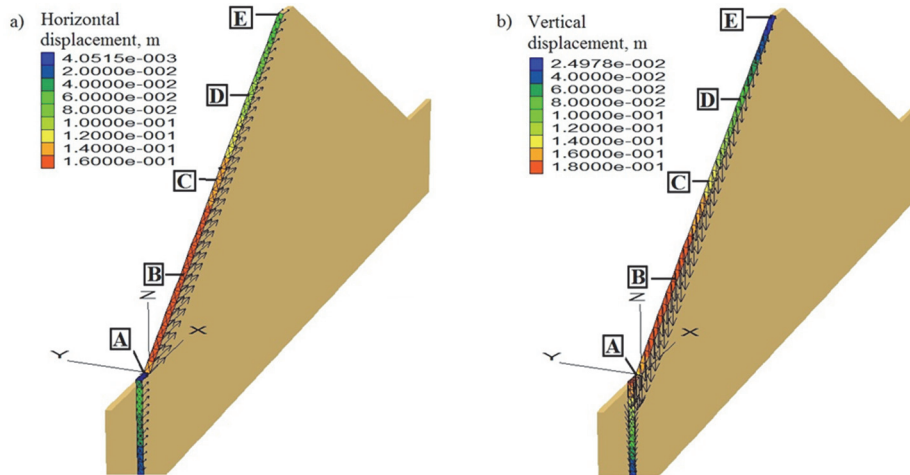


Figure 16. Horizontal (a) & vertical (b) displacements of concrete face after filling of the reservoir up to maximum elevation (CFRD of the 2nd stage, $H = 82$ m):

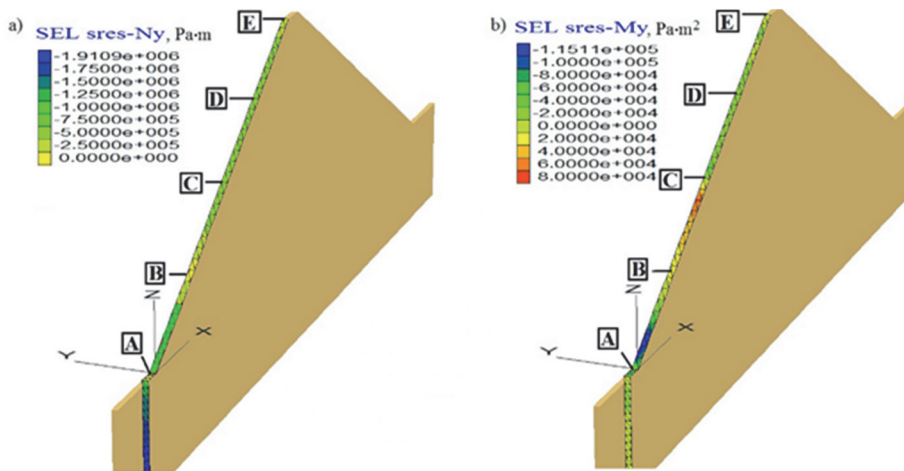


Figure 17. Longitudinal forces (a) and bending moments (b) in the concrete face after filling of the reservoir up to maximum elevation (CFRD of the 2nd stage, $H = 82$ m)

LEGEND FOR FIGURES 16 AND 17:

A – point on perimetral joint; B – intermedial point; C – point on the crest of dam of the 1st stage;
 A – point on perimetral joint; B – intermedial point; C – point on the crest of dam of the 2nd stage.

Displacements in points of concrete face:

A – $U_x = 0,14$ m; $U_z = -0,16$ m
 B – $U_x = 0,16$ m; $U_z = -0,18$ m
 C – $U_x = 0,14$ m; $U_z = -0,14$ m
 D – $U_x = 0,08$ m; $U_z = -0,10$ m
 E – $U_x = 0,06$ m; $U_z = -0,04$ m

Forces N & bending moments M in points of concrete face:

A – $N = -80$ t (compression); $M = -6$ tm
 B – $N = -40$ t (compression); $M = -2$ tm
 C – $N = -50$ t (compression); $M = 0$ tm
 D – $N = -50$ t (compression); $M = -2$ tm
 E – $N = -50$ t (compression); $M = -4$ tm

Deflections of concrete face: in point B (maximum) – 24 cm; in point C – 19 cm; in point D – 13 cm

4. Supposed designed behavior of the concrete face of Limon dam

From the pattern of deformations the behavior of concrete face acts as a rigid wall to vibrations in the transverse direction of the valley, differs considerably from the rockfill and transition zone materials, the transverse response across the valley of rockfill dam may be limited by the relatively rigid concrete face. This may lead to tension stresses in the plane of concrete face, seismic forces transferred from rockfill to concrete face are limited by the frictional forces between the transition zone of rockfill and concrete face. Like all the water load is supported by the concrete face, these frictional forces are relatively high and therefore stresses in the plane of concrete face can be significant enough to cause local deformations or shears of concrete face slabs along its longitudinal joints. The dam deformations can cause the crack opening in concrete slabs and sliding along the crack surface and suffer oscillating movements. This behavior of Limon dam corresponds to many case studies of behavior of concrete face rockfill dams, in detail described and discussed in [10–15].

The main advantage of this dam with concrete face is its high resistance to erosion in case of water seepage through cracked concrete face. If the zone of materials under the concrete face has a proper particle sizes the permeability coefficient will be 10^{-3} cm/s and then zone will be stable against its erosion. This eliminates the risk of high leakages developed under cracked concrete face.

Main conclusions

1. Horizontal and vertical displacements of the downstream slope after the Mar–Chile Earthquake are, respectively, 2.0–2.5 and 1–1.3 m. The maximum horizontal and vertical displacements of dam crest during the Mar–Chile Earthquake are, respectively, 1.5 and 1.1 m and after the earthquake – 0.4 and 0.3 m. These displacements about two times lower than those in the previous variant 1 of the dam with the downstream slope of ($V/H = 1/1.7$) and the under-laying rockfill without berms.

2. In comparison with the previous variant 1 of Limon dam ($H = 82$ m) with the downstream slope of ($V/H = 1/1.7$) and the under-laying rockfill without berms this variant 2 of Limon dam ($H = 82$ m) with additional gravel zone with two berms on downstream slope is much more stable and safe under action of very strong MCE of the Mar–Chile Earthquake. Therefore, this variant 2 of Limon dam can be adopted in the following detailed final design of 82 m high Limon dam.

3. During the forthcoming reservoir filling the strict monitoring of instruments embedded in dam body (piezometers, benchmarks, strain gauges, accelerometers) with expert control is necessary.

References

1. ICOLD Bulletin 148. (2010). *Selecting seismic parameters for large dams*. Guidelines.
2. ICOLD Bulletin 122. (2001). *Computational procedures for dam engineering*.
3. ICOLD Bulletin 154. (2011). *Dam safety management. Operational phase of the dam life cycle*.
4. ICOLD Bulletin 155. (2013). *Guidelines for use of numerical models in dam engineering*.
5. ICOLD Bulletin 167. (2015). *Regulation of dam safety. Overview of current practice*.
6. *Informe de gestión Proyecto Especial Olmos – Tinajones (PEOT)*. (Junio 2009).
7. *PLAXIS 2D PlaxFlow*. The Netherlands. <https://www.plaxis.com/product/plaxis-2d/>
8. *FLAC-3D software*. USA. <http://www.itascacg.com/>
9. *Proceedings of the ICOLD Congress*. (2003). Canada.
10. SPANCOLD. (1996). *Proceedings of the 4th Benchmark Workshop on Numerical Analysis of Dams*. Madrid, Spain.
11. USCOLD. (1999). *Proceedings of the 5th Benchmark Workshop on Numerical Analysis of Dams*. Denver, Colorado, USA.
12. ATCOLD and VERBUND. (2001). *Proceedings of the 6th Benchmark Workshop on Numerical Analysis of Dams*. Salzburg, Austria.
13. ROCOLD. (2003). *Proceedings of the 7th Benchmark Workshop on Numerical Analysis of Dams*. Bucharest, Romania.
14. Wuhan University. (2005). *Proceedings of the 8th Benchmark Workshop on Numerical Analysis of Dams*. Wuhan, China.
15. VNIIG (Russian Research Institute of Hydraulic Engineering named after B.E. Vedenev). (2007). *Proceedings of 9th Benchmark Workshop on Numerical Analysis of Dams*. Saint Petersburg, Russia.
16. COYNE ET BELLIER. (2009). *Proceedings of the 10th Benchmark Workshop on Numerical Analysis of Dams*. Gennevilliers, France.
17. Lyapichev Yu.P., Landau Yu.A. (November – December 2011). Modern structural and technological solutions for new large dams. *Hydro Review Worldwide*. PennWell Corp., USA.
18. Lyapichev Yu.P. (2013). Design, construction and behavior monitoring of modern high dams. Palmarium Academic, Germany, 369. (In Russ.)

About the author

Yury P. Lyapichev – Doctor of Technical Sciences, Professor, Expert of JSC “Hydroproject Institute” for foreign projects, Member of International Commission on

Large Dams (ICOLD). *Research interests*: dams, hydraulic structures (HS), static and seismic (dynamic) nonlinear analyses of rockfill and concrete dams, safety of dams and HS, elasto-plastic models of dam materials. *Contacts*: e-mail – lyapichev@mail.ru

For citation

Lyapichev Yu.P. (2019). Static and dynamic analyses of the heightening of concrete face gravel dam Limon (Peru). *Structural Mechanics of Engineering Constructions and Buildings*, 15(2), 158–168. DOI: 10.22363/1815-5235-2019-15-2-158-168

НАУЧНАЯ СТАТЬЯ

Статические и динамические расчеты наращивания грунтовой плотины с бетонным экраном Лимон (Перу)

Ю.П. Ляпичев

АО «Институт “Гидропроект”», Российская Федерация, 125993, Москва, Волоколамское шоссе, 2,
Международная комиссия по большим плотинам (ICOLD), France, 75016, Paris, Avenue Kleber, 61

Поступила в редакцию: 11 января 2019 г.
Доработана: 12 марта 2019 г.
Принята к публикации: 22 марта 2019 г.

Ключевые слова:

грунтовая плотина
с бетонным экраном (CFGD);
нелинейный сейсмический
(динамический) расчет;
ускорение основания;
акселерограмма землетрясения;
расчет фильтрации

Аннотация

Цели. Экспертная проверка предложенных проектных решений, разработка необходимых проектных решений по наращиванию плотины Лимон согласно рекомендациям ICOLD.

Методы. Подробные статические и сейсмические (динамические) расчеты напряженно-деформированного состояния (НДС) и фильтрации грунтовой плотины Лимон (Перу) с бетонным экраном были выполнены с использованием передовых программ численных расчетов FLAC-3D (США) и PLAXIS 2D (Голландия) соответственно. В статических и сейсмических (динамических) расчетах плотины Лимон использовалась упруго-пластическая модель Мора – Кулона с переменным углом сдвига гравийных и галечниковых зон плотины и грунтов ее основания. В динамических нелинейных расчетах НДС двух вариантов плотины Лимон при наполненном водохранилище использовалась акселерограмма максимального возможного землетрясения (МВЗ) Маг–Чиле.

Результаты. На основе полученных расчетов были разработаны рекомендации по проекту наращивания плотины с первоначальной высоты ($H = 43$ м) до 82 м перед первым наполнением водохранилища. Экспертная оценка всех необходимых проектных решений по наращиванию плотины Лимон была выполнена в соответствии с рекомендациями Международной комиссии по большим плотинам (ICOLD).

Список литературы

1. ICOLD Bulletin 148. Selecting seismic parameters for large dams. Guidelines. 2010.
2. ICOLD Bulletin 122. Computational procedures for dam engineering. 2001.
3. ICOLD Bulletin 154. Dam safety management. Operational phase of the dam life cycle. 2011.
4. ICOLD Bulletin 155. Guidelines for use of numerical models in dam engineering. 2013.
5. ICOLD Bulletin 167. Regulation of dam safety. Overview of current practice. 2015.
6. Informe de gestión Proyecto Especial Olmos – Tinajones (PEOT). Junio 2009.
7. PLAXIS 2D PlaxFlow. The Netherlands. <https://www.plaxis.com/product/plaxis-2d/>
8. FLAC-3D software. USA. <http://www.itascacg.com/>
9. Proceedings of the ICOLD Congress. Canada, 2003.
10. Proceedings of the 4th Benchmark Workshop on Numerical Analysis of Dams / SPANCOLD. Spain: Madrid, 1996.
11. Proceedings of the 5th Benchmark Workshop on Numerical Analysis of Dams / USCOLD. USA: Denver, Colorado, 1999.
12. Proceedings of the 6th Benchmark Workshop on Numerical Analysis of Dams / ATCOLD; VERBUND. Austria: Salzburg, 2001.
13. Proceedings of the 7th Benchmark Workshop on Numerical Analysis of Dams / ROCOLD. Romania: Bucharest, 2003.
14. Proceedings of the 8th Benchmark Workshop on Numerical Analysis of Dams / Wuhan University. China: Wuhan, 2005.
15. Proceedings of 9th Benchmark Workshop on Numerical Analysis of Dams / VNIIG (Russian Research Institute of Hydraulic Engineering named after B.E. Vedenev). Russia: Saint Petersburg, 2007.

16. Proceedings of the 10th Benchmark Workshop on Numerical Analysis of Dams / COYNE ET BELLIER. France: Gennevilliers, 2009.

17. Lyapichev Yu.P., Landau Yu.A. Modern structural and technological solutions for new large dams // Hydro Review Worldwide. November – December, 2011. USA: PennWell Corp. 12 p.

18. Ляпичев Ю.П. Проектирование, строительство и мониторинг поведения современных высоких плотин. Германия: Palmarium Academic, 2013. 369 с.

Об авторе

Ляпичев Юрий Петрович – доктор технических наук, профессор, эксперт по зарубежным проектам, АО «Институт Гидропроект», член Международной комис-

сии по большим плотинам (ICOLD). *Область научных интересов:* плотины, гидросооружения (ГС), статические и сейсмические (динамические) нелинейные расчеты грунтовых и бетонных плотин, безопасность плотин, упруго-пластические модели материалов плотин. *Контактная информация:* e-mail – lyapichev@mail.ru

Для цитирования

Lyapichev Yu.P. Static and dynamic analyses of the heightening of concrete face gravel dam Limon (Peru) (Статические и динамические расчеты наращивания грунтовой плотины с бетонным экраном Лимон (Перу)) // Строительная механика инженерных конструкций и сооружений. 2019. Т. 15. № 2. С. 158–168. DOI: 10.22363/1815-5235-2019-15-2-158-168